Non-viral, tumor-free induction of transient cell reprogramming in mouse skeletal muscle to enhance tissue regeneration

Short title: Transient reprogramming in mouse skeletal muscle

Irene de Lázaro[1,^,‡] , Acelya Yilmazer[1,$,^], Yein Nam[1], Sara Qubisi[1], Fazilah Maizatul Abdul Razak[1], Hans Degens[2], Giulio Cossu[3] and Kostas Kostarelos[1,*]

[1] *Nanomedicine Lab, Faculty of Biology, Medicine and Health, AV Hill Building, The University of Manchester, Manchester M13 9PT, United Kingdom; UCL School of Pharmacy, Faculty of Life Sciences, University College London (UCL), London WC1N 1AX United Kingdom*

[2] *School of Healthcare Science, Manchester Metropolitan University, John Dalton Building, Chester Street, Manchester, M1 5GD, United Kingdom*

[3] *Division of Cell Matrix Biology & Regenerative Medicine, Faculty of Biology, Medicine and Health, Michael Smith Building, The University of Manchester, Manchester M13 9PL, United Kingdom*

^ These authors contributed equally to this work

‡ Present address: Harvard School of Engineering and Applied Sciences, Cambridge, 02138 MA; Wyss Institute for Biologically Inspired Engineering, Harvard University, Boston, MA 02115, USA

$ Present address: Biomedical Engineering Department, Ankara University, 06830 Ankara, Turkey

* Correspondence should be addressed to K.K: kostas.kostarelos@manchester.ac.uk

Professor Kostas Kostarelos
AV Hill Building, University of Manchester
M13 9PT, Manchester, United Kingdom

Tel: +44 (0)161 275 1800

Abstract

Overexpression of *Oct3/4, Klf4, Sox2* and *c-Myc* (OKSM) transcription factors can de-differentiate adult cells *in vivo*. While sustained OKSM expression triggers tumorigenesis through uncontrolled proliferation of toti- and pluripotent cells, transient reprogramming induces pluripotency-like features and proliferation only temporarily, without teratomas. We sought to transiently reprogram cells within mouse skeletal muscle with a localized injection of plasmid DNA encoding OKSM (pOKSM) and hypothesized that the generation of proliferative intermediates would enhance tissue regeneration after injury. Intramuscular pOKSM administration rapidly upregulated pluripotency (*Nanog*, *Ecat1*, *Rex1*) and early myogenesis genes (*Pax3*) in the healthy gastrocnemius of various strains. Mononucleated cells expressing such markers appeared in clusters among myofibers, proliferated only transiently and did not lead to dysplasia or tumorigenesis for at least 120 days. *Nanog* was also upregulated in the gastrocnemius when pOKSM was administered 7 days after surgically sectioning its medial head. Enhanced tissue regeneration after reprogramming was manifested by the accelerated appearance of centro-nucleated myofibers and reduced fibrosis. These results suggest that transient *in vivo* reprogramming could develop into a novel strategy towards the acceleration of tissue regeneration after injury, based on the induction of transiently-proliferative, pluripotent-like cells *in situ*. Further research to achieve clinically meaningful functional regeneration is warranted.

Keywords: plasmid DNA, OKSM, *in vivo* reprogramming, pluripotency, muscle, regeneration

Introduction

Forced expression of *Oct3/4*, *Klf4*, *Sox2* and *cMyc* transcription factors, dubbed 'Yamanaka' or 'OKSM' reprogramming factors, reverts a wide variety of differentiated cell types to pluripotency, albeit with differing efficiencies[1-3]. Such conversion cannot only be triggered *in vitro* but also within living organisms[4-12]. *In vivo* cell reprogramming to pluripotency has been described in a variety of transgenic and wild-type (WT) animal models, in spite of pro-differentiation signals present in the tissue microenvironment, but with outcomes that vary depending on the pattern of OKSM overexpression[13]. Ubiquitous and/or sustained expression of reprogramming factors leads to uncontrolled proliferation of toti- and pluripotent cells and widespread tumorigenesis[6-11]. On the contrary, transient OKSM expression generates pluripotent intermediates that proliferate only temporarily, preventing dysplasia and teratoma formation[4, 5, 7, 12]. We proved this effect in WT mouse liver, using a non-viral approach based on hydrodynamic tail vein (HTV) injection of plasmid DNA (pDNA) encoding OKSM (pOKSM)[5, 12]. *In vivo* reprogrammed cells, also known as *in vivo* induced pluripotent stem (i^2PS) cells, demonstrated all main hallmarks of functional pluripotency[14]. Interestingly, other studies have shown that the frequency and duration of OKSM overexpression can be tuned to halt cell reprogramming at a proliferative but non-pluripotent stage that also avoids tumorigenesis[15, 16].

In the adult mammalian organism, muscle repair relies mainly on the self-renewal and myogenic potential of resident stem cells, primarily satellite cells[17]. The number and regenerative capacity of such cells varies across species and dramatically decreases with age[18, 19], hence it can be exhausted if the injury is severe or repeated, or occurs in elderly muscle. In such scenario, various resident cell types differentiate into myofibroblasts that generate a fibrotic scar unable to meet the

contractile requirements of the tissue, thus impeding the complete functional rehabilitation of the injured muscle[20, 21].

Different strategies are currently being explored to enhance muscle regeneration after severe injuries, including surgical suturing[22] or administration of anti-fibrotic drugs[20, 21, 23-25], growth factors[26], replacement cells[27-29], combinations of these[30-32] and miRNAs involved in muscle development[33]. However, none of these approaches has yet reached routine clinical practice and the treatment and management of major muscle injuries continues to be primarily conservative[34, 35]. At the same time, the skeletal muscle offers an excellent platform for the expression of foreign genes *in vivo*, given the capacity of myofibers and interstitial cells to uptake naked pDNA after a simple intramuscular (i.m.) administration[36, 37].

We have previously hypothesized that the generation of pluripotent or pluripotent-like cells *in vivo*, that are able to transiently proliferate and eventually re-differentiate to the appropriate phenotype within a damaged tissue, may assist its cellular repopulation boosting its capacity to regenerate after a traumatic insult or injury[38]. In the present work, we aimed first to explore whether transient, teratoma-free reprogramming could be achieved in mouse skeletal muscle via i.m. administration of pOKSM. We then interrogated whether cell reprogramming would enhance the regenerative capacity of the muscle after a surgically-induced injury.

Results

Gene expression in mouse skeletal muscle after i.m. administration of reprogramming factors.

To test whether the expression of pluripotency-related genes could be induced by OKSM in mouse skeletal muscle, we first administered BALB/c mice with 50 μg of a single pDNA cassette, pOKSM, that encodes OKSM factors and a GFP reporter, in the gastrocnemius (GA). The

contralateral hind limb was injected with the same volume of saline solution and used as control (**Figure 1a**). Changes in gene expression in the GA were investigated at different time points after injection by real-time RT-qPCR (**Figure 1b-d**). 2 days after injection, *Sox2 and c-Myc* mRNAs were significantly upregulated in muscles administered with pOKSM, compared to saline-injected controls (p= 0.043 for *Sox2*, p=0.035 for *cMyc*). However, by day 4 we did not observe significant differences between groups (**Figure 1b**). *Oct3/4* and *GFP* expression was not detected in saline-injected muscles, therefore relative expression was normalised to the values of pOKSM-injected muscles dissected on day 2. We observed a significant decrease in the levels of both mRNAs from day 2 to day 4 after injection (p=0.003 for *Oct3/4*, p=0.042 for *GFP*) and none of such targets were amplified at a later time point (day 8 after injection, **Figure 1b**).

Nanog, *Ecat1* and *Rex1* are genes expressed in the pluripotent state but repressed in adult tissues. Significant upregulation of these pluripotency markers was confirmed as early as 2 days after pOKSM administration (p=0.021 for *Nanog*, p=0.034 for *Ecat1* and p=0.04 for *Rex1*). Similar to the trend observed in the expression of reprogramming factors, their mRNA levels decreased afterwards (**Figure 1c**). In addition, we investigated the expression of genes characteristically expressed at different stages during myogenesis. Higher mRNA levels of *Pax3* — expressed in myogenic progenitors, but not in differentiated myofibers[39] — were detected in the pOKSM injected group. On the contrary, *MyoD1,* that is expressed in more committed cells during skeletal muscle development[40] and is directly suppressed by *Oct4* during myoblast-to-iPS cell reprogramming[41], was expressed at lower levels compared to saline-injected controls (**Figure 1d**). Again, these changes persisted only transiently.

To confirm that the above changes in pluripotency and myogenesis markers were indeed triggered by OKSM and not by the injection of pDNA itself, we also administered BALB/c mice

with 50 μg pGFP. This cassette encoded a GFP reporter, but no OKSM factors (**Figure S1a**). As expected, *Oct3/4* mRNA was not amplified by real-time RT-qPCR and *Sox2* and *cMyc* were expressed at the same levels as saline-injected controls (**Figure S1b**). In addition, the expression of pluripotency (**Figure S1c**) and myogenesis-related genes remained unaltered (**Figure S1d**). GFP mRNA levels remained stable for the duration of the study (8 days, **Figure S1e**).

Taken together, the changes in gene expression observed in pOKSM-injected tissues were compatible with a transient reprogramming event, whereby forced OKSM expression could activate an embryonic-like gene expression program, inducing the expression of pluripotency but also early myogenesis markers, in a subset of cells within the tissue.

Identification of reprogrammed cells within muscle tissue. The analysis of mRNA from bulk tissue did not allow to determine whether the changes in the transcripts described above occurred in the same cells, nor to identify the specific cell subsets within the tissue that undertook reprogramming. Besides, the rapid decline in transgene mRNA levels upon pOKSM injection contrasted with the stable and long-term foreign gene expression that is normally observed after the uptake of pDNA in post-mitotic myofibers[42]. To clarify this, and to overcome the limitations of bulk tissue RNA analysis, we obtained muscle tissue sections 2 and 4 days after pDNA administration and identified transfected cells based on the expression of the GFP reporter (**Figure 1e**). *Nanog* is considered the archetypic marker of pluripotency[43] and was significantly upregulated in pOKSM-injected muscles **(Figure 1c)**, thus we utilized an anti-NANOG antibody to distinguish reprogrammed cells within the skeletal muscle tissue. Interestingly, green fluorescence was found in both myofibers (**Figure S2b**) and interstitial mononucleated cells located among muscle fibers (**Figure 1e**), but we observed significant differences between pOKSM and pGFP-injected tissues. In

pOKSM-injected muscles, 2 days after injection, some of such GFP^+ interstitial cells were located in large cell clusters that stained positively for NANOG (**Figure 1e**). However, the overall number of GFP^+ cell clusters (**Figure 1f**) and, especially, that of $NANOG^+GFP^+$ double positive cell clusters, decreased significantly by day 4 in this group ($p=0.03$ and $p=0.0002$, respectively, **Figure 1e-g**). The number of GFP^+ cell clusters in pGFP-injected tissues did not change in such time frame ($p=0.62$). This observation agrees with our mRNA data on transgene and pluripotency marker expression (**Figure 1b-c** and **Figure S2e**) and could be explained if transient reprogramming induced cell division with the consequent loss of the transfected plasmid. Of note, this vector is known to remain mainly as an episome[44].

NANOG was only found in pOKSM-injected tissues, always within clusters of GFP^+ mononucleated cells among myofibers (**Figure 1e**). This observation further confirmed that the upregulation of the pluripotency marker was triggered by OKSM overexpression. It is to note that not all GFP^+ cells within $NANOG^+GFP^+$ clusters expressed NANOG, and that some GFP^+ cell clusters in pOKSM injected tissues contained no $NANOG^+$ cells at all (**Figure 1e-g**). Considering the well-known low efficiency of cell reprogramming, even under more controlled *in vitro* conditions[44], this result was expected. **Figure S3** shows further details of representative $NANOG^+GFP^+$ cell clusters found on pOKSM-injected tissues, including orthogonal views that confirm $NANOG^+GFP^+$ co-localisation. The expression of NANOG was cytoplasmic, instead of its most common localization in the cell nucleus. However, such event has been previously described by others[45, 46]. NANOG was not detected from day 4 after i.m. injection (**Figure 1e and 1f**), which supported our observations at the mRNA level and confirmed that de-differentiation to a pluripotent-like state occurred only transiently.

The expression of a GFP gene product can trigger a mild immune cell reaction, albeit significant differences have been found among mouse strains and depending on the route of administration[47]. We aimed to rule out the possibility that the large $NANOG^+GFP^+$ cell clusters observed in pOKSM-injected tissues corresponded in fact to the recruitment of immune cells around the needle tract left by the i.m. injection. First, we confirmed that no NANOG expression was detected around the needle tract in saline-injected and pGFP-injected muscles (**Figure S2c**). In addition, we found an average 8.5 ± 0.7 $NANOG^+/GFP^+$ cell clusters per GA and those were distributed in proximal and distal areas from the injection site (**Figure 1g**). We also ruled out the possibility that pOKSM resulted more immunogenic than pGFP or saline injection comparing mRNA levels of *Cd11b* — a leucocyte marker — among saline, pGFP and pOKSM-injected muscles. We did not find significant differences among such groups (**Figure S2d**). Staining pOKSM-injected tissues with an anti-CD11b antibody confirmed that a number of $CD11b^+$ cells were present within $NANOG^+GFP^+$ cell clusters, however CD11b and NANOG expression did not co-localize in the same cells (**Figure S2e**). This may indicate that immune cells are recruited to the sites of $NANOG^+GFP^+$ cell clusters but confirms that their identity is different from that of reprogrammed cells.

***In vivo* reprogramming in Nanog-GFP and Pax3-GFP transgenic mice skeletal muscle.** Sv129-Tg(Nanog-GFP) transgenic mice, referred to as Nanog-GFP for simplicity, have the reporter GFP sequence inserted in the *Nanog* locus[43]. They were used to identify cells exhibiting pluripotency-like features in the tissue, thanks to the emission of green fluorescence. pOKS and pM plasmids, containing the OKSM reprogramming factors in two separate cassettes, were used instead of pOKSM to avoid overlap with the GFP reporter encoded in the latter (**Figure 2a**). Prior to any

histological analysis, we confirmed that the expression of reprogramming factors, endogenous pluripotency genes and myogenesis-related markers on days 2, 4 and 8 after i.m. injection was comparable to that observed in WT mice (**Figure 2b-d**). As in the BALB/c strain, gene expression changes in Nanog-GFP mice GA suggested the reprogramming of a subset of cells within the muscle towards an embryonic-like state (**Figure 2c-d**).

In addition, we aimed to clarify the input of pericytes and satellite cells, since they are present in the skeletal muscle and have myogenic potential[17, 48]. Especially, satellite cells express *Pax3* in certain muscles[39]. Therefore, it was of particular importance to rule out the contribution of a hypothetical satellite cell proliferative response, which could be triggered by the injection trauma, towards the elevated mRNA levels of such transcription factor. With that aim, we investigated the expression of other satellite cell-specific markers (*Pax7, Caveolin1, Integrin-α7, Jagged1*) and pericyte markers (*TN-AP, Pdgfrβ, Rgs5*). A significant reduction of their mRNA levels was found in pOKSM-injected specimens compared to controls (**Figure 2 e-f**), which ruled out an injection-induced proliferation of such cell types but rather pointed at them as potential targets of reprogramming.

At the histological level (**Figure 3**), H&E staining revealed the presence of dense clusters of mononucleated cells among the myofibers in Nanog-GFP mice administered with OKSM. The bright green fluorescence observed 2 days after injection (**Figure 3b**) that confirmed the expression of *Nanog* and hence the pluripotent-like identity of such cells, was not detected at later time points (data not shown), which further confirmed the transiency of reprogramming. An average of 6.3 ± 1.3 GFP^+ clusters were identified per GA, in agreement with the number of $NANOG^+$ clusters quantified in the BALB/c study (**Figure 1g**). In addition, GFP co-localised with the expression of several other pluripotency and embryonic stem cell specific markers identified by IHC (NANOG,

OCT4, AP and SSEA1) (**Figure 3c**). The number of cell clusters positive for such markers is shown in **Figure S4** and was in a similar order. No GFP signal or immunoreactivity for any of the pluripotency markers tested was found in saline-injected controls, excluding alkaline phosphatase (AP), which is also expressed by pericytes (**Figure S5b and d**).

We also found cells staining positively for satellite cell and pericyte markers (PAX7 and PDGFrβ, respectively) within GFP^+ cell clusters. However, similar to what we observed when we investigated the presence of immune cells in reprogrammed tissues, such cells did not express the green fluorescence characteristic of reprogrammed cells (**Figure S5c**). This observation confirmed that the appearance of large clusters of mononucleated cells within reprogrammed tissues was not due to proliferation of satellite cells or pericytes, at least in the absence of a prior reprogramming event.

We then used the CBA-Tg(Pax3-GFP) transgenic mouse strain[49], shortened as Pax3-GFP, to confirm the upregulation of the early myogenesis marker *Pax3*. 2 days after the injection of pOKS and pM, we found and average of 7 ± 1.4 GFP^+ cell clusters per GA, similar to the number of GFP^+ cell clusters observed in Nanog-GFP mouse tissues from the same treatment group (**Figure 3b**). Green fluorescence did not appear in saline-injected controls (**Figures S5b**). In addition, the staining of an anti-NANOG antibody in OKSM-injected tissues co-localised with the green fluorescence signal triggered by PAX3 expression (**Figure 3d**). This finding confirmed that reprogrammed cells expressing NANOG also expressed PAX3.

Overall, these data suggested that cells reprogrammed within the skeletal muscle tissue grew in clusters among myofibers and expressed pluripotency and early myogenic progenitor markers. While not all cells within the clusters in Nanog-GFP and Pax3-GFP specimens expressed the green reporter, this heterogeneity may again be explained by the limited efficiency of the reprogramming

process. Taking also into account the transiency of the reprogramming event, we cannot rule out that some of such cells were already re-differentiating at the time point investigated (day 2). The occurrence of partial reprogramming events that do not reach the de-differentiation status of $NANOG^{+}PAX3^{+}$ cells may also be considered.

Short and long-term effects of *in vivo* reprogramming in healthy skeletal muscle. We next focused on the outcome of OKSM-mediated reprogramming in healthy BALB/c GA with an emphasis on signs of cell proliferation and of the potential appearance of dysplastic lesions or teratomas. Both short and long time points after reprogramming — from day 2 to 120 after pOKSM injection — were studied (**Figure 4a-b**). We first sought to obtain more stringent evidence of cell proliferation within the reprogrammed cell clusters, given that cell division is known as a distinct and indispensable step in the somatic-to-pluripotent conversion[50, 51]. 18 h after i.m. administration of 50 μg pOKSM or saline control, BALB/c mice were i.p. injected with 5-Bromo-2'deoxyuridine (BrdU), which can be incorporated in the DNA of proliferating cells[52]. Tissues were collected 6 h later for histological examination (**Figure 4a**). GA tissue sections were stained with an anti-BrdU antibody, while the eGFP reporter in pOKSM was used to identify the cells transfected with reprogramming factors. We found co-localisation of the two signals in cell clusters within the GA tissue in pOKSM-injected mice, which were morphologically identical to those observed in our previous studies. This finding confirmed that *in vivo* reprogrammed cells not only acquired an embryonic-like gene expression profile, but also proliferated actively.

We then followed the evolution of such clusters in the reprogrammed tissues (**Figure 4b**). While they were very densely populated by small mononucleated cells on day 2 after injection, from day 4, small calibre, desmin-positive, centronucleated myofibers (characteristic features of

regenerating, immature myofibers[53, 54]) started to predominate instead. By day 8, only few desmin-positive, centronucleated myofibers remained, and none were noted at later time points (**Figure 4c-d**). Lower magnification images of these observations are shown in **Figure S6b**. Very importantly, no teratomas or any signs of tissue abnormality were observed for the duration of the study (120 days). This observation, together with the progressive disappearance of cell clusters, suggests that the proliferative state confirmed by BrdU incorporation (**Figure 4a**) was only transient.

TUNEL staining indicated the presence of limited numbers of apoptotic nuclei in the GA tissue. However, those were only found at the earliest time points after injection (day 2) and in both conditions (saline and pOKSM injection); hence their occurrence was attributed to the mild tissue damage caused by the injection along the needle tract (**Figure S6c**). The absence of significant cell death constitutes a first indication that *in vivo* reprogrammed cells could successfully re-integrate into the muscle tissue. In the absence of an appropriate lineage tracing system, we next performed morphometric analyses to indirectly follow the fate of reprogrammed cells. The distribution of myofiber diameter shifted to larger calibers compared to saline-injected controls (**Figure 4e**), whereas the average number of myofibers per cross-sectional area remained unaltered (**Figure 4f**). These data could indicate that reprogrammed cells proliferate in clusters to then fuse with existing myofibers, enlarging their diameter, but do not form *de novo* fibers. If confirmed, this course of events would recapitulate those that occur during post-natal myogenesis[55]. Nonetheless, *ad hoc* lineage tracing studies must in the future be employed to confirm these findings.

Enhancement of regeneration in a surgically-induced model of skeletal muscle injury. The capacity of *in vivo* reprogramming to enhance regeneration was interrogated in a clinically relevant model of skeletal muscle injury. The medial head of the left GA of BALB/c mice was surgically

sectioned in the transverse plane (as represented in **Figure S7a)** and pOKSM was i.m. administered in the injured hind limb at the time of injury, 5 or 7 days later. We chose such timings so that significant endogenous regeneration would have not yet taken place, thus to explore if *in vivo* reprogramming would accelerate the process, and to look for differences in the induction of reprogramming at different stages of muscle degeneration. Control mice bearing the same injury were injected with 0.9% saline solution alone and the contralateral (right) leg of each mouse was left intact (uninjured and uninjected) as internal control. The analysis of *Nanog* mRNA levels in the tissue 2 days after administration of pOKSM revealed that maximum upregulation of the pluripotency marker was achieved when the Yamanaka factors were administered 7 days after injury (**Figure S7b**). We thus selected such dose regime for further studies, whereby muscle regeneration was investigated 9 and 14 days after injury (2 and 7 days after administration of reprogramming factors or saline control) (**Figure 5a**). The uptake and expression of the reprogramming pDNA, evidenced by *Oct3/4* expression, was confirmed on day 9. mRNA levels of the transgene were significantly higher in the lateral head of the GA compared to the directly injured medial head ($p=0.027$), possibly due to the abundance of necrotic myofibers at the injury site. Similarly, the higher mRNA levels of *Nanog* were detected in the lateral head of the GA ($p=0.010$ compared to saline control, **Figure 5b**).

H&E staining confirmed the loss of normal muscle tissue architecture and its replacement by granulation tissue with high degree of cellularity — most likely composed of interspersed inflammatory cells, among others — in the vicinity of the injury. Signs of mineralization (deeply basophilic deposits) and neovascularization were also observed. All such histological aberrations were evident in both groups on day 9 after injury but diminished considerably by day 14 in reprogrammed tissues (**Figure 5c**). Laminin/DAPI staining allowed the quantification of

centronucleated myofibers (**Figure 5d**). On day 9, a higher percentage of myofibers surrounding the injured site were regenerating in the reprogrammed group (56.0 ± 23.4%) — as evidenced by the centralised position of the nucleus — compared to saline controls (33.9 ± 12.9%), p= 0.005. In the saline-injected group, the percentage of centronucleated myofibers continued to increase (45.6 ± 14.6% on day 14), an indication that the regeneration process was still ongoing. On the contrary, the number of regenerating fibers decreased significantly by day 14 in *in vivo* reprogrammed tissues (18.2 ± 7.7% 14, p=0.0001 compared to day 9). The formation of a fibrotic scar is one of the hallmarks of muscle remodelling after injury that prevents the functional rehabilitation of the tissue[20, 21]. We investigated whether the administration of reprogramming factors would have any effect on the deposition of collagen after injury and found that collagen-positive areas (detected by picrosirius red/fast green staining) on day 9 were more extensive in the tissues from saline-control animals (p=0.029), such difference being more significant on day 14 (p=0.0001). Between these two time points, the fibrotic area (calculated as a percentage of the total area in the cross-section) in the vicinity of the injury increased only slightly (12.3 ± 5.1% to 15.5 ± 6.5%, p=0.012) in the OKSM-injected group. In contrast, the area of fibrotic tissue increased significantly, from 15.4 ± 5.2% on day 9 to 22.6 ± 6.7% on day 14, in mice that received saline only (p=0.000, **Figure 5e**).

Finally, we tested whether the improvements observed at the histological level would translate into a significant improvement in muscle function in the sectioned GA. The recovery of muscle force was measured by *in vivo* myography 9 and 14 days after injury (**Figure S8a**). In brief, the GA and sciatic nerve were exposed in terminally anaesthetized mice and connected to a myograph as shown in **Figure S8b,** so that muscle force under twitch and tetanus contractions was measured upon direct stimulation of the nerve. Fast-twitch was produced by a single stimulation at optimal voltage and length, and isometric tensile strength was recorded (**Figure S8c**). Tetanus

contraction was produced by a series of stimulations repeated with a frequency of 150 Hz (**Figure S8d**). 7 days after i.m. administration of reprogramming pDNA (14 days after injury), treated animals recovered a higher percentage of the force of the contralateral (intact) leg as compared to saline-injected controls, when both fast twitch (50.4 ± 12.3% for saline, 80.2 ± 18.2% for OKSM injected animals) and tetanus (49.9 ± 19.2% for saline, 56.6 ± 20.9% for OKSM injected animals) contractions were investigated. However, none of such differences were statistically significant (**Figure S8e-f**).

Discussion

This study demonstrates that the induction of transient cell reprogramming within the skeletal muscle tissue — accompanied by likewise transient proliferation — accelerates regeneration at the histological level in a model of severe muscle injury. Our laboratory was first to report *in vivo* cell reprogramming to pluripotency in an adult mammalian tissue (liver) via forced expression of OKSM factors[5, 12, 14]. Here, transient expression of the same factors in healthy adult skeletal muscle also rapidly triggered the upregulation of pluripotency markers that are otherwise repressed in adult tissues (**Figure 1c** and **Figure 2c**). With the data obtained here we cannot confirm whether reprogrammed cells within the skeletal muscle reached a state of functional pluripotency, as we found in our previous work[14], hence we have referred to them as "reprogrammed" or "pluripotent-like" cells. In fact, co-expression of PAX3, a marker of myogenic precursors, in the same cells that expressed the pluripotency marker NANOG suggests that OKSM overexpression could have induced a partial reprogramming event in this tissue (**Figure 3d**). A recent work by Ocampo *et al* also described the induction of partial reprogramming when OKSM expression was not sustained for long periods of time[15]. In such study, reprogrammed cells did not activate the

expression of pluripotency-related genes, such as *Nanog*, but they did proliferate. As in our study, proliferation was only transient and no teratomas were found within reprogrammed tissues. We have previously pointed at the duration of OKSM expression as a critical factor to avoid tumorigenesis upon *in vivo* reprogramming and therefore to preserve the potential of this technology to develop into a therapeutic strategy[13]. The observations that we have made in the present study support our previous claims[5, 12] and Ocampo's[15] that teratoma-free *in vivo* cell reprogramming can be achieved when OKSM expression is limited in time.

Intramuscular injection of pDNA has been previously reported to result in long-term transgene expression that can last for 2 months and reach peak levels 14 days after injection, based on the post-mitotic status of muscle fibers[42]. This contrasted with the rapid decrease in the expression of the transfected reprogramming factors observed in our study (**Figure 1b** and **Figure 2b**), which we explain by the proliferative status of pOKSM-transfected cells evidenced by BrdU labelling (**Figure 4a**) and by the predominantly episomal state of the pDNA vectors utilised in this stud, which can thus be lost with cell division[44]. BrdU incorporation was found within GFP^+ cell clusters in reprogrammed tissues but not in saline-injected controls and therefore proliferation was attributed to the reprogramming event. Indeed, active cell division is an early and mandatory step in the differentiated-to-pluripotent conversion[51]. This finding also suggested that *in vivo* reprogramming could enhance the cellular repopulation of a tissue after injury, precisely by increased cell proliferation. In addition, our histological observations of the evolution of the reprogrammed cell clusters over time suggested that, after the proliferative phase, reprogrammed cells re-differentiated and successfully re-integrated in the muscle tissue (**Figure 4b-f** and **Figure S4**). This was supported by the gradual disappearance of mononucleated cell clusters, the rapid decrease in the expression of pluripotency markers, together with the emergence of desmin-positive

centronucleated myofibers from days 4 to 8 after injection, enlargement of myofiber diameter and the absence of pronounced apoptosis and of dysplastic lesions or teratomas. Nonetheless, despite the consistency among these observations, specific lineage tracing studies that allow permanent labelling of *in vivo* reprogrammed cells must be pursued in the future to confirm this hypothesis and confidently determine the fate of reprogrammed cells within the tissue. We also noted that centralised nuclei persisted only for up to 8 days after injection, which differs from classic regeneration where such feature is observed for longer periods of time[17].

One of the caveats in our study remains the elucidation of the specific cell types that are reprogrammed within the skeletal muscle tissue, a limitation that affects most of the *in vivo* reprogramming studies published to date, regardless of the target tissue[5-7, 11, 15]. The multinucleated and post-mitotic status of muscle fibers would require cell fission and cell cycle re-entry to achieve successful reprogramming towards a pluripotent-like state. While myofibers of urodele amphibians de-differentiate and cleave into mononucleated progenitors during regeneration[56], there is currently no evidence that mammalian myofibers can undergo such processes. Recent studies attempted to achieve mammalian myofiber de-differentiation and fission via ectopic expression of transcription factors that mediate such processes in amphibians[57-59] or via muscle injury[60, 61]. However, they also lacked robust lineage tracing tools that could confirm the origin of the resulting mononucleated cells. Here, we confirmed the expression of the GFP reporter encoded in pOKSM in both myofibers and mononucleated interstitial cells, but NANOG was only co-expressed in the latter (**Figure 1e** and **Figure S2b**). This observation suggests that OKSM expression may not be able to induce cell reprogramming in differentiated myofibers. Myoblasts have however been successfully de-differentiated into iPS cells *in vitro* via *Oct4*-mediated *MyoD1* downregulation[41, 62]. Interestingly, we consistently observed a decrease in *MyoD1* mRNA levels in the reprogrammed groups

throughout our study (**Figure 1d** and **Figure 2d**). We also confirmed downregulation of markers specific to satellite cells. *In vitro*, these cells have shown to be more efficiently reprogrammed than other more committed cell types[62]. In addition, a report from Chiche *et al* that also explored the *in vivo* induction of pluripotency in the mouse skeletal muscle, identified $PAX7^+$ satellite cells as the major cell of origin of reprogrammed cells within such tissue. However, the contribution of other cell types was not investigated[10]. In our study, given the probably random incorporation of pDNA in a variety of cells and the absence of cell type-specific promoters in the cassettes, it is conceivable that different interstitial cells were reprogrammed rather than a specific cell type, all down-regulating their differentiated markers.

We have previously hypothesized that generation of transiently proliferative, pluripotent-like cells in the context of an injured tissue might help its cellular repopulation and overall regeneration[38]. Indeed, there are notorious limitations in the management of major skeletal muscle injuries, for which the clinically-established treatment continues to be conservative and the often lack of complete recovery leads to fibrosis and loss of muscle contractility[63]. In our study, the administration of pDNA encoding Yamanaka factors 7 days after severe muscle injury not only accelerated the recovery towards normal muscle architecture (**Figure 5c**) and the appearance of centronucleated myofibers (**Figure 5d**), but also induced a moderate decrease of collagen deposition compared to the control group (**Figure 5e**). During the peer-review process of this manuscript, Doeser and colleagues found similar observations upon induction of transient reprogramming with OKSM factors in cutaneous wounds. *In vivo* reprogramming reduced the levels of profibrotic markers (*Tgfβ-1*, *Collagen I* and *Vegf*) and resulted in reduced scar formation at the wound site. *α-Sma* expression, associated to myofibroblast proliferation, was also significantly diminished in comparison to control (non-reprogrammed) wounds[16]. It is thus conceivable that the reduced

fibrosis observed in Doeser's and our own study is, at least partly, due to an OKSM-induced decrease in post-injury fibroblast-to-myofibroblast transdifferentiation.

In our hands, the histological improvements above did not translate into significant differences in the recovery of muscle force (**Figure S8**). In fact, only the administration of anti-fibrotic drugs has demonstrated significant functional rehabilitation in mouse injury models of comparable severity[20, 23]. Other strategies, including administration of adipose-derived stem cells and surgical suturing, reported improvements at the histological level only[32], similar to us, or utilized milder injury models[22, 31]. Thus, future work is warranted to identify optimal gene transfer vectors and dosage regimes that grant clinically-relevant, functional rehabilitation upon *in vivo* reprogramming. Indeed, transfection efficiency following i.m. administration of pDNA is relatively low and highly variable[64] and, *in vitro*, use of naked pDNA to force OKSM overexpression has shown lower reprogramming efficiency compared to other alternatives, especially viral vectors[65]. This agrees with our observation that not all pOKSM-transfected cells within reprogrammed tissues expressed NANOG (**Figure 1e** and **Figure S3**). Other strategies in the current literature may have achieved higher *in vivo* reprogramming efficiencies but lack clinical relevance based on the use of transgenic mouse models[6, 15] or retroviral vectors that cause genomic integration of OKSM transgenes, followed by sustained reprogramming and tumorigenesis[8]. We thus foresee that the search of appropriate gene transfer vectors that boost the efficiency of *in vivo* reprogramming without compromising the safety of the approach (i.e. preserving the transiency of reprogramming) will be a main priority for the field.

The teratoma-free approach that we have postulated in this work may also offer advantages to other reprogramming-based strategies. First, it bypasses the need for *ex vivo* manipulation and transplantation, and their associated risks, encountered by the *in vitro* generation of induced

pluripotent stem (iPS) cells. Such limitations have been exhaustively reviewed by others[66, 67]. The presence of a transient proliferative stage (**Figure 4a**) offers a possibility for cellular expansion and repopulation that *in vivo* transdifferentiation strategies described to date (i.e. direct reprogramming between two differentiated cell types, avoiding pluripotent intermediates and active cell division) lack[68-76]. In addition, transdifferentiation strategies require the identification of specific reprogramming factors to mediate each particular cell type conversion, while pluripotency can be induced in a variety of starting cell types with the defined OKSM cocktail [1, 2, 77].

Abundant necrosis and neutrophil infiltration occurs rapidly (1-2 days) after muscle injury and is followed by prominent macrophage recruitment and secretion of cytokines and damage signals, among them IL-6, for up to approximately the first week after injury [78]. An interesting finding in our work is that *Nanog* upregulation was significantly higher when pOKSM was administered 7 days after injury, compared to earlier interventions (**Figure S7b**). This observation agrees with recent findings by Mosteiro et al.[11] and Chiche et al.[10], which demonstrated that signals of tissue damage and senescence, among which IL-6 plays a key role, promote reprogramming by boosting cell plasticity. Ocampo et al. also found that the efficiency or reprogramming increased in senescent tissues[15]. Thus, it is conceivable that in our study reprograming was compromised at the very early time points after injury, given the abundance of cells becoming necrotic, but on the contrary was favoured by the later peak of inflammation and release of IL-6 by day 7 after injury. Regardless of the mechanism, this observation adds a further advantage to the potential use of *in vivo* reprogramming to enhance tissue regeneration, as reprogramming appears to be favoured within injured and/or aged tissues. Besides, the synergy between damage and reprogramming in this time-frame circumvents the need for a rapid post-injury intervention. This is indeed a caveat of many muscle regeneration experimental strategies, especially of cell based therapies that are

administered at the time of injury, while the time required to achieve sufficient cell numbers for implantation can reach several weeks[27, 28, 31, 32].

We have proposed here a transient reprogramming strategy to generate pluripotent-like intermediates *in situ* that can assist cellular repopulation of an injured tissue while circumventing the challenges faced by cell transplantation — including cell isolation, extensive culturing and the inherent risk of genomic aberrations, delivery and engraftment. We hypothesize that this strategy could benefit from the presence of differentiation cues in the tissue microenvironment able to re-differentiate the *in vivo* reprogrammed cells to the appropriate phenotypes. The transient character of this approach has proved critical to avoid tumorigenesis, a burden that keeps other *in vivo* reprogramming to pluripotency strategies far from the road into the clinic.

Materials and Methods

DNA plasmids (pDNA). pCX-OKS-2A (pOKS), encoding Oct3/4, Klf4, Sox2; pCX-cMyc (pM), encoding cMyc, and pCAG-GFP (pGFP), encoding GFP, all under control of the constitutive CAG promoter, were purchased as bacterial stabs from Addgene (USA). pLenti-lll-EF1a-mYamanaka (pOKSM), encoding Oct3/4, Klf4, Sox2, cMyc and GFP under control of the constitutive EF1α promoter, was purchased from Applied Biological Materials (USA). Research grade plasmid production was performed in Plasmid Factory (Germany).

Animals. All experiments were performed with prior approval from the UK Home Office under a project license (PPL 70/7763) and in strict compliance with the Guidance on the Operation of the Animals (Scientific Procedures) Act 1986. BALB/c mice were purchased from Harlan (UK).

Sv129-Tg(Nanog-GFP) mice, which carry the GFP reporter inserted into the *Nanog* locus [43], were a kind gift from the Wellcome Trust Centre for Stem Cell Research, University of Cambridge (UK) and bred in heterozygosity and genotyped at the University of Manchester. CBA-Tg(Pax3-GFP), in which GFP replaces the *Pax3* coding sequence of exon 1 [49], were bred and genotyped at the University of Manchester. All mice used in this work were female of 7 weeks of age. Mice were allowed one week to acclimatize to the animal facilities prior to any procedure.

Intramuscular (i.m.) administration of pDNA. Mice were anesthetised with isofluorane and the left gastrocnemius (GA) was injected with either 50 µg pOKSM, 50 µg pGFP or 50 µg pOKS and 50 µg pM in 50 µl 0.9% saline solution. The contralateral (right) leg was injected with 50 µl 0.9% saline solution alone as internal control. Mice were culled at different time points, including 2, 4, 8, 12, 24, 50 and 120 days after i.m. injection, as specified in each particular study.

RNA isolation and real-time RT-qPCR analysis. Aurum Fatty and Fibrous Kit (Bio-rad, UK) was used to isolate total RNA from muscle tissue. cDNA synthesis from 1 µg of RNA sample was performed with iScript cDNA synthesis kit (Bio-Rad, UK) according to manufacturer's instructions. 2 µl of each cDNA sample were used to perform real-time RT-qPCR reactions with iQ SYBR Green Supermix (Bio-Rad, UK). Primer sequences are shown in **Supplementary Table 1**. Experimental duplicates were run on CFX-96 Real Time System (Bio-Rad, UK) with the following protocol: 95°C for 3 min, 1 cycle; 95°C for 10 sec, 60°C for 30 sec, – repeated for 40 cycles. *β-actin* was used as a housekeeping gene and gene expression levels were normalised to saline-injected controls, unless otherwise specified, following the Livak ($2^{\wedge-\Delta\Delta Ct}$) method. RT-qPCR data is presented as median $2^{\wedge-\Delta\Delta CT}$ ± propagation of the error from Ct values. ACt values were used for statistical analysis.

Immunohistochemistry (IHC) of BALB/c muscle tissue sections. GA were dissected 2 and 4 days after i.m. injection with pOKSM, pGFP, or saline control and immediately frozen in isopentane, pre-cooled in liquid nitrogen. 10 μm-thick sections (in the transverse plane) were prepared on a cryostat (Leica, CM3050S) and air-dried for 1 h at room temperature (RT) prior to storage at -80°C. Before staining, muscle sections were post-fixed with methanol, pre-cooled at -20°C, for 10 min, air-dried for 15 min and finally washed twice with PBS for 5 min. Sections were then incubated for 1 h in blocking buffer (5% goat serum-0.1% Triton in PBS pH 7.3) at RT, followed by two washing steps with PBS (1 %BSA- 0.1% Triton, pH 7.3) and overnight incubation at +4°C with primary antibodies: rabbit pAb anti-NANOG (ab80892, 1/200, Abcam, UK) and chicken pAb anti-GFP (ab13970, 1/1000, Abcam, UK). The next day, sections were washed twice (5 min each) with PBS and incubated (1.5 h, RT) with secondary antibodies: goat polyclonal anti-rabbit IgG labeled with Cy3 (1/250, Jackson ImmunoResearch Laboratories.) and goat polyclonal anti-chicken IgY labeled withAlexa-647 (1/500, ab150171, Abcam, UK). After two washes in PBS, slides were mounted with ProLong® Gold anti-fade DAPI containing medium (Life Technologies, UK). Whole muscle sections were imaged with a 3D Histech Pannoramic 250 Flash slide scanner. The number of GFP^+ and $NANOG^+GFP^+$ cell clusters and the number of GFP^+ muscle fibers was counted in n=2 GA, 3 sections per muscle. Representative images were taken at 20X magnification with Pannoramic Viewer software. Z stacks and orthogonal views (**Figure S2e** and **Figure S3**) were obtained at 100X magnification with a Leica TCS SP5 AOBS inverted confocal microscope.

Characterisation of GFP^+ cell clusters in Nanog-GFP and Pax3-GFP transgenic mice. To characterize the clusters of reprogrammed cells in Nanog-GFP and Pax3-GFP mice, GA were administered with pOKS and pM vectors, to avoid overlapping of the GFP reporter in pOKSM, and sacrificed 2 and 4 days after injection. To observe the GFP signal, frozen tissue sections obtained as

described before were simply mounted with ProLong® Gold anti-fade DAPI containing mountant (Life Technologies, UK) after fixation and imaged with 3D Histech Pannoramic 250 Flash slide scanner. The number of GFP^+ clusters was counted from n=4 GA. Representative images (100X) were taken with Panoramic Viewer. To investigate co-localisation of the GFP signal with the expression of different markers, tissue sections were processed for IHC as described above. Rabbit pAb anti-OCT4 (ab19857,3 µg/ml, Abcam, UK), rabbit pAb anti-NANOG (ab80892, 1 µg/ml, Abcam, UK), rabbit pAb anti-AP (ab95462, 1:200, Abcam, UK), mouse mAb anti-SSEA1 (ab16285, 20 µg/ml, Abcam, UK), rabbit pAb anti-Pax7 (pab0435, 1:200, Covalab, France), and rabbit mAb anti-PDGFrβ (3169, 1:100, Cell Signalling) were used as primary antibodies. Anti-PDGFrβ was a kind gift from Prof. Cossu's lab (University of Manchester). Goat pAb anti-rabbit IgG labeled with Cy3 and goat pAb anti-mouse IgG labeled with Cy5 (1/250, Jackson ImmunoResearch Laboratories) were used as secondary antibodies. Images were taken at 100X magnification with a Leica TCS SP5 AOBS inverted confocal microscope.

Histological evaluation of muscle tissue. BALB/c GA were dissected on days 2, 4, 8, 15, 50 and 120 after i.m. injection with pOKSM or saline control, frozen and sectioned as previously described. H&E staining was performed following a standard protocol. Tissue sections were imaged with a 3D Histech Pannoramic 250 Flash slide scanner and representative images at 40X and 100X magnification were taken with Pannoramic Viewer software. The minimum myofiber diameter and number of myofibers/cross-sectional area were analysed from 5 sections per muscle (n=3 GA per condition and time point), with ImageJ 1.48 software.

Desmin/laminin/DAPI staining. 10 µm-thick cryosections were stained following the IHC protocol previously described, using rabbit pAb anti-laminin (ab11575, 1:200, Abcam, UK) and mouse mAb anti-desmin (ab6322, 1:200, Abcam, UK) as primary antibodies. Goat pAb anti-rabbit IgG labeled

with Cy3 (1/250, Jackson ImmunoResearch Laboratories) and goat pAb anti-mouse IgG labeled with Cy5 (1/250, Jackson ImmunoResearch Laboratories) were used as secondary antibodies. 40X images were obtained with a Zeiss Axio Observer epi-Fluorescence microscope.

BrdU labelling and detection of proliferating cells. BrdU assay was used to label proliferating cells *in vivo*, as previously described [79]. BALB/c mice were intraperitoneally (i.p.) administered with 500mg/kg of 5-Bromo-2'-deoxyuridine (BrdU, B5002, Sigma, UK) in 0.9% saline 18 h after i.m. injection with pOKSM or saline control. 6 h later, GA were dissected and processed for IHC as described above. Treatment with 2 N HCl (10 min at 37°C) after fixation was performed to denature the DNA. Mouse mAb anti-BrdU (B8434, 1:100, Sigma, UK) and goat pAb anti-mouse IgG labeled with Cy5 (1/250, Jackson ImmunoResearch Laboratories) were used.100X images were captured with a Leica TCS SP5 AOBS inverted confocal microscope.

Surgically-induced skeletal muscle injury model and *in vivo* reprogramming to pluripotency. BALB/c mice were anesthetised with isoflurane and the left hind limb was shaved and prepared for surgery. 0.05 mg/kg buprenorphine was subcutaneously (s.c.) administered at the start of the intervention. A vertical skin incision (6 mm long) was made overlying the posterior compartment of the calf with a scalpel number 11 and the fascia was exposed and incised with fine scissors at the level of mid-gastrocnemius to release the muscle belly. The medial head of the GA was blunt dissected (i.e. carefully separated from the lateral head and remaining fascia without cutting or damaging the tissue) and sectioned at its mid-point with a single incision, performed with a scalpel number 11, in the transverse plane. The medial head was sectioned in its full width and depth, as described in **Figure S7a**. The sural nerve and lateral head of the GA were preserved. The skin was sutured with 5 interrupted stitches (Vicryl 6-0 absorbable suture, Ethicon, UK) and mice were allowed to recover in a warm chamber. The contralateral (right) leg was left intact for internal

control. 7 days after surgery 100 μg pOKSM in 40 μl 0.9% saline or 40 μl 0.9% saline alone were i.m. administered in the injured (left) leg. The contralateral (right) leg was left uninjected. Mice were sacrificed at days 9 and 14 after injury (2 and 7 days after pOKSM or saline administration) for histological and electromechanical investigations (n=4). A group of animals was also culled at day 9 (day 2 after i.m. injection) for gene expression analysis.

Laminin/DAPI staining and analysis of % of centronucleated myofibers. 10 μm-thick cryosections were obtained 9 and 14 days after surgical transection and IHC stained following the protocol previously described using rabbit pAb anti-laminin (ab11575, 1:200, Abcam, UK) and goat pAb anti-rabbit IgG labeled with Cy3 (1/250, Jackson ImmunoResearch Laboratories) antibodies. Whole muscle sections were imaged with 3D Histech Pannoramic 250 Flash slide scanner and 63X captures of random fields were collected with Pannoramic Viewer Software. The number of centronucleated myofibers and total number of fibers per cross-sectional area were quantified using ImageJ 1.48 software from 3 randomly selected fields per section. The data for each mouse were calculated from 2 sections (one from each half of the transected GA, close to the site of injury) and we observed 4 mice in each group. Measurements and calculations were conducted in a blinded manner.

Picrosirius red-fast green staining and analysis of fibrotic area. GA were dissected 9 and 14 days after injury and fixed in 10% buffered formalin solution (Sigma, UK). Tissues were embedded in paraffin wax and 5 μm thick sagittal and transverse sections obtained with a microtome (Leica RM2255) were left to dry overnight at 37°C prior to the staining procedure. Tissue sections were de-paraffinized following a standard protocol and stained for 1 h in picrosirius red/fast green staining solution (0.1% Sirius red, 0.1% fast green in a saturated aqueous solution of picric acid). Tissue sections were then quickly immersed in 0.5% acetic acid for 6 s, dehydrated in 100% ethanol

and xylene to be finally mounted with DPX (Sigma, UK). Sections were imaged on a 3D Histech Pannoramic 250 Flash slide scanner and 40X images were obtained with Pannoramic Viewer Software. The percentage of collagen-positive areas was quantified with ImageJ 1.48 software in 5 randomly selected fields per section. The data for each mouse were calculated from 2 sections (one from each half of the transected GA, close to the site of injury) and 4 mice were included per group. Measurements and calculations were conducted in a blinded manner.

Sample size calculations. Sample size for gene expression studies was determined based on differences in *Nanog* expression in prelimary studies, given its hallmark role in cell reprogramming. We calculated sample size taking into account the means and standard deviations of *Nanog* ΔCt for control and OKSM-treated mice, power = 80% and Type I error =0.05, and considering a one-way ANOVA comparison between the means. We also utilised the results observed in a previous work from our group[5], which explored the *in vivo* induction of pluripotency in mouse liver via the same episomal plasmid system, to inform the design and sample size determination of the studies in this work.

Statistical analysis. N numbers were specified for each particular study. Statistical analysis was performed first by Levene's test to assess homogeneity of variance. When no significant differences were found in the variances of the different groups, statistical analysis was followed by one-way ANOVA and Tukey's post-hoc test. When variances were unequal, the analysis was followed with Welch ANOVA and Games-Howell's post-hoc test. Probability values <0.05 were regarded as significant. SPSS software version 20.0 was used to perform this analysis.

Author contributions

IdL, AY and KK conceived the project and designed experiments. IdL and AY performed the majority of experiments. SQ contributed to some qPCR data. YN and FR performed some IHC experiments. HD helped to set up *in vivo* myography. GC advised in experimental design and interpretation of data. IdL, AY, GC and KK wrote the manuscript.

Acknowledgements

IdL and KK are the recipients of an award by the Royal College of Surgeons of Edinburgh (grant KAE WONJ4). IdL would like to thank Obra Social LaCaixa and UCL School of Pharmacy for a jointly funded PhD Studentship. The authors would also like to acknowledge the Histology and Bioimaging Facilities at the University of Manchester for assistance, as well as Dr Adam Reid (University of Manchester) for his help in the establishment of the injury model utilised in this study.

Disclosure/Conflict of interests

The authors declare no conflicts of interest.

References

1. Takahashi, K., and Yamanaka, S. (2006). Induction of pluripotent stem cells from mouse embryonic and adult fibroblast cultures by defined factors. *Cell* **126**: 663-676.
2. Aoi, T., *et al.* (2008). Generation of pluripotent stem cells from adult mouse liver and stomach cells. *Science* **321**: 699-702.
3. Okita, K., *et al.* (2013). An efficient nonviral method to generate integration-free human-induced pluripotent stem cells from cord blood and peripheral blood cells. *Stem Cells* **31**: 458-466.
4. Vivien, C., Scerbo, P., Girardot, F., Le Blay, K., Demeneix, B.A., and Coen, L. (2012). Non-viral expression of mouse Oct4, Sox2, and Klf4 transcription factors efficiently reprograms tadpole muscle fibers in vivo. *J Biol Chem* **287**: 7427-7435.
5. Yilmazer, A., de Lazaro, I., Bussy, C., and Kostarelos, K. (2013). In vivo cell reprogramming towards pluripotency by virus-free overexpression of defined factors. *PLoS One* **8**: e54754.
6. Abad, M., *et al.* (2013). Reprogramming in vivo produces teratomas and iPS cells with totipotency features. *Nature* **502**: 340-345.
7. Ohnishi, K., *et al.* (2014). Premature Termination of Reprogramming In Vivo Leads to Cancer Development through Altered Epigenetic Regulation. *Cell* **156**: 663-677.
8. Gao, X., Wang, X., Xiong, W., and Chen, J. (2016). In vivo reprogramming reactive glia into iPSCs to produce new neurons in the cortex following traumatic brain injury. *Scientific reports* **6**: 22490.
9. Choi, H.W., Kim, J.S., Hong, Y.J., Song, H., Seo, H.G., and Do, J.T. (2015). In vivo reprogrammed pluripotent stem cells from teratomas share analogous properties with their in vitro counterparts. *Scientific reports* **5**: 13559.
10. Chiche, A., *et al.* (2017). Injury-Induced Senescence Enables In Vivo Reprogramming in Skeletal Muscle. *Cell Stem Cell*.
11. Mosteiro, L., *et al.* (2016). Tissue damage and senescence provide critical signals for cellular reprogramming in vivo. *Science* **354**.
12. Yilmazer, A., de Lazaro, I., Bussy, C., and Kostarelos, K. (2013). *In vivo* reprogramming of adult somatic cells to pluripotency by overexpression of Yamanaka factors. *JoVE* **17**.
13. de Lazaro, I., Cossu, G., and Kostarelos, K. (2017). Transient transcription factor (OSKM) expression is key towards clinical translation of in vivo cell reprogramming. *EMBO Mol Med*.
14. de Lazaro, I., Bussy, C., Yilmazer, A., Jackson, M.S., Humphreys, N.E., and Kostarelos, K. (2014). Generation of induced pluripotent stem cells from virus-free in vivo reprogramming of BALB/c mouse liver cells. *Biomaterials* **35**: 8312-8320.
15. Ocampo, A., *et al.* (2016). In Vivo Amelioration of Age-Associated Hallmarks by Partial Reprogramming. *Cell* **167**: 1719-1733 e1712.
16. Doeser, M.C., Scholer, H.R., and Wu, G. (2018). Reduction of Fibrosis and Scar Formation by Partial Reprogramming In Vivo. *Stem Cells*.
17. Charge, S.B., and Rudnicki, M.A. (2004). Cellular and molecular regulation of muscle regeneration. *Physiol Rev* **84**: 209-238.
18. Allbrook, D.B., Han, M.F., and Hellmuth, A.E. (1971). Population of muscle satellite cells in relation to age and mitotic activity. *Pathology* **3**: 223-243.
19. Blau, H.M., Cosgrove, B.D., and Ho, A.T. (2015). The central role of muscle stem cells in regenerative failure with aging. *Nature medicine* **21**: 854-862.

20. Fukushima, K., Badlani, N., Usas, A., Riano, F., Fu, F., and Huard, J. (2001). The use of an antifibrosis agent to improve muscle recovery after laceration. *Am J Sports Med* **29**: 394-402.
21. Sato, K., *et al.* (2003). Improvement of muscle healing through enhancement of muscle regeneration and prevention of fibrosis. *Muscle Nerve* **28**: 365-372.
22. Menetrey, J., Kasemkijwattana, C., Fu, F.H., Moreland, M.S., and Huard, J. (1999). Suturing versus immobilization of a muscle laceration. A morphological and functional study in a mouse model. *Am J Sports Med* **27**: 222-229.
23. Chan, Y.S., *et al.* (2003). Antifibrotic effects of suramin in injured skeletal muscle after laceration. *J Appl Physiol (1985)* **95**: 771-780.
24. Foster, W., Li, Y., Usas, A., Somogyi, G., and Huard, J. (2003). Gamma interferon as an antifibrosis agent in skeletal muscle. *J Orthop Res* **21**: 798-804.
25. Negishi, S., Li, Y., Usas, A., Fu, F.H., and Huard, J. (2005). The effect of relaxin treatment on skeletal muscle injuries. *Am J Sports Med* **33**: 1816-1824.
26. Menetrey, J., *et al.* (2000). Growth factors improve muscle healing in vivo. *J Bone Joint Surg Br* **82**: 131-137.
27. Natsu, K., Ochi, M., Mochizuki, Y., Hachisuka, H., Yanada, S., and Yasunaga, Y. (2004). Allogeneic bone marrow-derived mesenchymal stromal cells promote the regeneration of injured skeletal muscle without differentiation into myofibers. *Tissue Eng* **10**: 1093-1112.
28. Shi, M., *et al.* (2009). Acceleration of skeletal muscle regeneration in a rat skeletal muscle injury model by local injection of human peripheral blood-derived CD133-positive cells. *Stem Cells* **27**: 949-960.
29. Mori, R., *et al.* (2012). Promotion of skeletal muscle repair in a rat skeletal muscle injury model by local injection of human adipose tissue-derived regenerative cells. *J Tissue Eng Regen Med*.
30. Lee, C.W., *et al.* (2000). BIOLOGICAL INTERVENTION BASED ON CELL AND GENE THERAPY TO IMPROVE MUSCLE HEALING AFTER LACERATION. *Journal of Musculoskeletal Research* **04**: 265-277.
31. Park, J.K., *et al.* (2012). Losartan improves adipose tissue-derived stem cell niche by inhibiting transforming growth factor-beta and fibrosis in skeletal muscle injury. *Cell Transplant* **21**: 2407-2424.
32. Hwang, J.H., Kim, I.G., Piao, S., Jung, A.R., Lee, J.Y., and Park, K.D. (2013). Combination therapy of human adipose-derived stem cells and basic fibroblast growth factor hydrogel in muscle regeneration. *Biomaterials* **34**: 6037-6045.
33. Nakasa, T., Ishikawa, M., Shi, M., Shibuya, H., Adachi, N., and Ochi, M. (2010). Acceleration of muscle regeneration by local injection of muscle-specific microRNAs in rat skeletal muscle injury model. *J Cell Mol Med* **14**: 2495-2505.
34. Gharaibeh, B., *et al.* (2012). Biological approaches to improve skeletal muscle healing after injury and disease. *Birth Defects Res C Embryo Today* **96**: 82-94.
35. Maffulli, N., *et al.* (2013). ISMuLT Guidelines for muscle injuries. *Muscles Ligaments Tendons J* **3**: 241-249.
36. Wolff, J.A., *et al.* (1990). Direct gene transfer into mouse muscle in vivo. *Science* **247**: 1465-1468.
37. Dupuis, M., *et al.* (2000). Distribution of DNA vaccines determines their immunogenicity after intramuscular injection in mice. *J Immunol* **165**: 2850-2858.

38. de Lazaro, I., and Kostarelos, K. (2014). In vivo cell reprogramming to pluripotency: exploring a novel tool for cell replenishment and tissue regeneration. *Biochemical Society Transactions* **42**: 711-716.
39. Collins, C.A., *et al.* (2009). Integrated functions of Pax3 and Pax7 in the regulation of proliferation, cell size and myogenic differentiation. *PLoS One* **4**: e4475.
40. Buckingham, M. (2006). Myogenic progenitor cells and skeletal myogenesis in vertebrates. *Curr Opin Genet Dev* **16**: 525-532.
41. Watanabe, S., *et al.* (2011). MyoD gene suppression by Oct4 is required for reprogramming in myoblasts to produce induced pluripotent stem cells. *Stem Cells* **29**: 505-516.
42. Wolff, J.A., Ludtke, J.J., Acsadi, G., Williams, P., and Jani, A. (1992). Long-term persistence of plasmid DNA and foreign gene expression in mouse muscle. *Hum Mol Genet* **1**: 363-369.
43. Chambers, I., *et al.* (2007). Nanog safeguards pluripotency and mediates germline development. *Nature* **450**: 1230-1234.
44. Okita, K., Hong, H., Takahashi, K., and Yamanaka, S. (2010). Generation of mouse-induced pluripotent stem cells with plasmid vectors. *Nat Protoc* **5**: 418-428.
45. Ye, F., Zhou, C.Y., Cheng, Q., Shen, J.J., and Chen, H.Z. (2008). Stem-cell-abundant proteins Nanog, Nucleostemin and Musashi1 are highly expressed in malignant cervical epithelial cells. *Bmc Cancer* **8**.
46. Elatmani, H., Dormoy-Raclet, V., Dubus, P., Dautry, F., Chazaud, C., and Jacquemin-Sablon, H. (2011). The RNA-Binding Protein Unr Prevents Mouse Embryonic Stem Cells Differentiation Toward the Primitive Endoderm Lineage. *Stem Cells* **29**: 1504-1516.
47. Skelton, D., Satake, N., and Kohn, D.B. (2001). The enhanced green fluorescent protein (eGFP) is minimally immunogenic in C57BL/6 mice. *Gene Ther* **8**: 1813-1814.
48. Sirabella, D., Angelis, L., and Berghella, L. (2013). Sources for skeletal muscle repair: from satellite cells to reprogramming. *J Cachexia Sarcopenia Muscle* **4**: 125-136.
49. Relaix, F., Rocancourt, D., Mansouri, A., and Buckingham, M. (2005). A Pax3/Pax7-dependent population of skeletal muscle progenitor cells. *Nature* **435**: 948-953.
50. Buganim, Y., *et al.* (2012). Single-Cell Expression Analyses during Cellular Reprogramming Reveal an Early Stochastic and a Late Hierarchic Phase. *Cell* **150**: 1209-1222.
51. Buganim, Y., Faddah, D.A., and Jaenisch, R. (2013). Mechanisms and models of somatic cell reprogramming. *Nat Rev Genet* **14**: 427-439.
52. Veronese, S., Gambacorta, M., and Falini, B. (1989). In situ demonstration of tissue proliferative activity using anti-bromo-deoxyuridine monoclonal antibody. *J Clin Pathol* **42**: 820-826.
53. Buckingham, M., *et al.* (2003). The formation of skeletal muscle: from somite to limb. *J Anat* **202**: 59-68.
54. Koch, U., Lehal, R., and Radtke, F. (2013). Stem cells living with a Notch. *Development* **140**: 689-704.
55. White, R.B., Bierinx, A.S., Gnocchi, V.F., and Zammit, P.S. (2010). Dynamics of muscle fibre growth during postnatal mouse development. *BMC Dev Biol* **10**: 21.
56. Morrison, J.I., Loof, S., He, P., and Simon, A. (2006). Salamander limb regeneration involves the activation of a multipotent skeletal muscle satellite cell population. *J Cell Biol* **172**: 433-440.
57. Odelberg, S.J., Kollhoff, A., and Keating, M.T. (2000). Dedifferentiation of mammalian myotubes induced by msx1. *Cell* **103**: 1099-1109.

58. McGann, C.J., Odelberg, S.J., and Keating, M.T. (2001). Mammalian myotube dedifferentiation induced by newt regeneration extract. *Proc Natl Acad Sci U S A* **98**: 13699-13704.
59. Yang, Z., *et al.* (2014). Mononuclear cells from dedifferentiation of mouse myotubes display remarkable regenerative capability. *Stem Cells* **32**: 2492-2501.
60. Miyoshi, T., Nakano, S., Nakamura, K., Yamanouchi, K., and Nishihara, M. (2012). In vivo electroporation induces cell cycle reentry of myonuclei in rat skeletal muscle. *J Vet Med Sci* **74**: 1291-1297.
61. Mu, X., Peng, H., Pan, H., Huard, J., and Li, Y. (2011). Study of muscle cell dedifferentiation after skeletal muscle injury of mice with a Cre-Lox system. *PLoS One* **6**: e16699.
62. Tan, K.Y., Eminli, S., Hettmer, S., Hochedlinger, K., and Wagers, A.J. (2011). Efficient generation of iPS cells from skeletal muscle stem cells. *PLoS One* **6**: e26406.
63. Baoge, L., *et al.* (2012). Treatment of skeletal muscle injury: a review. *ISRN Orthop* **2012**: 689012.
64. Andre, F.M., Cournil-Henrionnet, C., Vernerey, D., Opolon, P., and Mir, L.M. (2006). Variability of naked DNA expression after direct local injection: the influence of the injection speed. *Gene Ther* **13**: 1619-1627.
65. Mochiduki, Y., and Okita, K. (2012). Methods for iPS cell generation for basic research and clinical applications. *Biotechnol J* **7**: 789-797.
66. Forsberg, M., and Hovatta, O. (2012). Challenges for the Therapeutic use of Pluripotent Stem Derived Cells. *Front Physiol* **3**: 19.
67. Lowry, W.E., and Quan, W.L. (2010). Roadblocks en route to the clinical application of induced pluripotent stem cells. *J Cell Sci* **123**: 643-651.
68. Banga, A., Akinci, E., Greder, L.V., Dutton, J.R., and Slack, J.M. (2012). In vivo reprogramming of Sox9+ cells in the liver to insulin-secreting ducts. *Proc Natl Acad Sci U S A* **109**: 15336-15341.
69. Qian, L., *et al.* (2012). In vivo reprogramming of murine cardiac fibroblasts into induced cardiomyocytes. *Nature* **485**: 593-598.
70. Song, K., *et al.* (2012). Heart repair by reprogramming non-myocytes with cardiac transcription factors. *Nature* **485**: 599-604.
71. Jayawardena, T.M., *et al.* (2012). MicroRNA-mediated in vitro and in vivo direct reprogramming of cardiac fibroblasts to cardiomyocytes. *Circ Res* **110**: 1465-1473.
72. Inagawa, K., *et al.* (2012). Induction of cardiomyocyte-like cells in infarct hearts by gene transfer of Gata4, Mef2c, and Tbx5. *Circ Res* **111**: 1147-1156.
73. Guo, Z., Zhang, L., Wu, Z., Chen, Y., Wang, F., and Chen, G. (2014). In vivo direct reprogramming of reactive glial cells into functional neurons after brain injury and in an Alzheimer's disease model. *Cell Stem Cell* **14**: 188-202.
74. Heinrich, C., *et al.* (2014). Sox2-mediated conversion of NG2 glia into induced neurons in the injured adult cerebral cortex. *Stem Cell Reports* **3**: 1000-1014.
75. Su, Z., Niu, W., Liu, M.L., Zou, Y., and Zhang, C.L. (2014). In vivo conversion of astrocytes to neurons in the injured adult spinal cord. *Nat Commun* **5**: 3338.
76. Jayawardena, T.M., *et al.* (2015). MicroRNA induced cardiac reprogramming in vivo: evidence for mature cardiac myocytes and improved cardiac function. *Circ Res* **116**: 418-424.
77. Zhang, X.B. (2013). Cellular Reprogramming of Human Peripheral Blood Cells. *Genomics Proteomics Bioinformatics*.

78. Huard, J., Li, Y., and Fu, F.H. (2002). Muscle injuries and repair: current trends in research. *J Bone Joint Surg Am* **84-A**: 822-832.
79. Curran, J. (2001). In Vivo Assay of Cellular Proliferation. vol. 174. pp 379-389.

Figure Captions

Figure 1. Changes is gene and protein expression after i.m. administration of reprogramming pDNA in mouse GA. (a) BALB/c mice were i.m. injected in the GA with 50 µg pOKSM or pGFP in 50 µl 0.9% saline, or with 50 µl saline alone. GA were dissected 2, 4 and 8 days after injection with pOKSM or saline and real-time RT-qPCR was performed to determine changes in gene expression of **(b)** reprogramming factors and GFP transgene encoded in pOKSM, **(c)** endogenous pluripotency markers and **(d)** genes involved in myogenesis. Gene expression levels were normalised to day 2 for *Oct3/4* and *GFP* mRNA. **p<0.01 and *p<0.05 indicate statistically significant differences between day 2 and day 4 p.i., assessed by one-way ANOVA, n.a. indicates no amplification of the target. Expression levels of other transcripts were normalised to saline-injected controls and *p<0.05 indicates statistically significant differences in gene expression between pOKSM and saline-injected groups, assessed by one-way ANOVA or Welch ANOVA. Data are presented as 2^-ΔΔCt ± propagated error, n=3. **(e)** 10 µm-thick GA sections obtained 2 or 4 days after saline, pOKSM or pGFP injection were stained with anti-NANOG and anti-GFP antibodies. Images were taken with a slide scanner at 20X magnification, scale bars represent 50µm. **(f)** Number of GFP^+ cell clusters per GA. *p<0.05 and **p<0.01 indicate statistically significant differences in the number of GFP^+ clusters compared to saline-injected controls and ^{s}p<0.05 indicates statistically significant differences between 2 and 4 days after pOKSM injection, assessed by one-way ANOVA and Tukey test, (n=2 GA, 3 (whole) sections/muscle). **(g)** Number of

$NANOG^+/GFP^+$ cell clusters per GA. ***p<0.001 indicates statistically significant differences in the number of $NANOG^+/GFP^+$ clusters between pOKSM injected muscles (2 days p.i.) and the rest of the groups, assessed by one-way ANOVA and Tukey's test, (n=2 GA, 3 whole sections/muscle).

Figure 2. Changes in gene expression after i.m. administration of reprogramming pDNA in Nanog-GFP mice. (a) Nanog-GFP transgenics were i.m. administered 50 μg pOKS and 50 μg pM in 50 μl 0.9% saline, or 50 μl saline alone, in the GA. 2, 4 and 8 days p.i. GA tissues were dissected, and real-time RT-qPCR was performed to determine the relative gene expression of **(b)** reprogramming factors, **(c)** endogenous pluripotency markers, **(d)** genes involved in myogenesis, **(e)** satellite cell markers and **(f)** pericyte markers. Relative expression was normalised to day 2 values (*Oct3/4* and *GFP* mRNAs) or to saline-injected controls (other genes). *p<0.05 and **p<0.01 indicate statistically significant differences in gene expression between pDNA and saline-injected groups, assessed by one-way ANOVA or Welch ANOVA. Data are presented as 2^-ΔΔCt ± propagated error, n=4.

Figure 3. Characterisation of *in vivo* reprogrammed cell clusters in the GA of Nanog-GFP and Pax3-GFP mice. (a) Nanog-GFP and Pax3-GFP transgenics were administered 50 μg pOKS and 50 μg pM in 50 μl 0.9% saline in the GA, dissected 2 days p.i. for histological analysis. **(b)** Clusters of reprogrammed cells were identified by H&E and the green fluorescence resulting from either *Nanog* or *Pax3* upregulation (100X, scale bars represent 50 μm). Bright field and fluorescence images show the same region within the tissue. *p<0.05 and ***p<0.001 indicate statistically significant differences in the number of GFP^+ clusters found in reprogrammed tissues, compared to saline-injected controls, assessed by one-way ANOVA, n=4 (Nanog-GFP mice) and n=2 (PAX3-GFP

mice). **(c)** IHC for the expression of pluripotency markers in Nanog-GFP GA administered with reprogramming pDNA, (100X, scale bars represent 50 μm). **(d)** IHC for NANOG expression in Pax3-GFP GA administered with reprogramming pDNA, (100X, scale bars represent 50 μm). *p<0.05 indicates statistically significant differences in the number of $NANOG^{+}/PAX3^{+}$ clusters found in reprogrammed tissues, compared to saline-injected controls, one-way ANOVA, n=2, 5 whole sections/muscle.

Figure 4. The effect of *in vivo* reprogramming towards pluripotency on healthy skeletal muscle. (a) BALB/c mice were administered 50 μg pOKSM in 50 μl 0.9% saline or 50 μl saline alone in the GA. 18 h later, BALB/c mice were administered 500mg/kg BrdU, i.p. GA were dissected 24 h after pDNA injection. 10 μm-thick tissue sections were stained with anti-BrdU antibody. Green fluorescence corresponds to the GFP reporter encoded in the pDNA. Images were captured with a confocal microscope (100X). Scale bar represents 50 μm. **(b)** BALB/c mice were administered 50 μg pOKSM in 50 μl 0.9% saline or 50 μl saline alone in the GA. Muscles were dissected 2, 4, 8, 12, 50 and 120 days p.i., sectioned and stained with **(c)** H&E (100X, scale bar represents 50 μm) and **(d)** anti-desmin and anti-laminin antibodies (40X, scale bar represents 50 μm). **(e)** Fiber size distribution. *p<0.05 indicates statistically significant differences in the frequency of 70 μm fibers between pOKSM and saline-injected groups, analysed by one-way ANOVA, n=3, data are presented as mean ± SD. **(f)** Number of myofibers per cross section. No statistically significant differences were found between pOKSM and saline-injected animals, analysed by one-way ANOVA, n=3, data are presented as mean ± SD.

Figure 5. The effect of *in vivo* reprogramming towards pluripotency after laceration of the medial head of the GA. (a) The medial head of the GA of BALB/c mice was surgically transected and 100 μg pOKSM in 40 μl 0.9% saline, or 40 μl saline alone, were i.m. administered 7 days after surgery. GA muscles were dissected 9 and 14 days after injury. **(b)** *Oct3/4* and *Nanog* gene expression was normalised to saline-injected controls. *p<0.05 indicates statistically significant differences between *Oct3/4* expression in the medial and lateral heads of the GA of pDNA injected mice and in the *Nanog* expression between the lateral head of the GA of pDNA and saline-injected animals, assessed by one-way ANOVA and Tukey's test, n=4. **(c)** H&E staining (40X, scale bar represents 100μm). Orange arrowheads point at sites of likely neovascularization. Green arrowheads point at areas of likely mineralization. Black dash-lines delineated areas of randomly organized regenerating myofibers. **(d)** Laminin/DAPI staining (63X, scale bar represents 50 μm) and quantification of % centronucleated myofibers. **p<0.01 and ***p<0.001 indicate statistically significant differences between pDNA and saline-injected groups and different time points, assessed by Welch ANOVA and Games Howell's test, (n=4 GA per group, 2 sections per muscle, 3 random fields per section). All data are presented as mean ± SD and numerical values are provided in **Table S2**. **(e)** Picrosirius red – fast green staining (40X, scale bar represents 100 μm) and measurement of areas with collagen deposition. *p<0.05 and ***p<0.001 indicate statistically significant differences between pDNA and saline-injected groups and different time points, assessed by one-way ANOVA and Tukey's test (n=4 GA per group, 2 sections per muscle, 5 random fields per section). All data are presented as mean ± SD and numerical values are provided in **Table S3**.

Figure 1

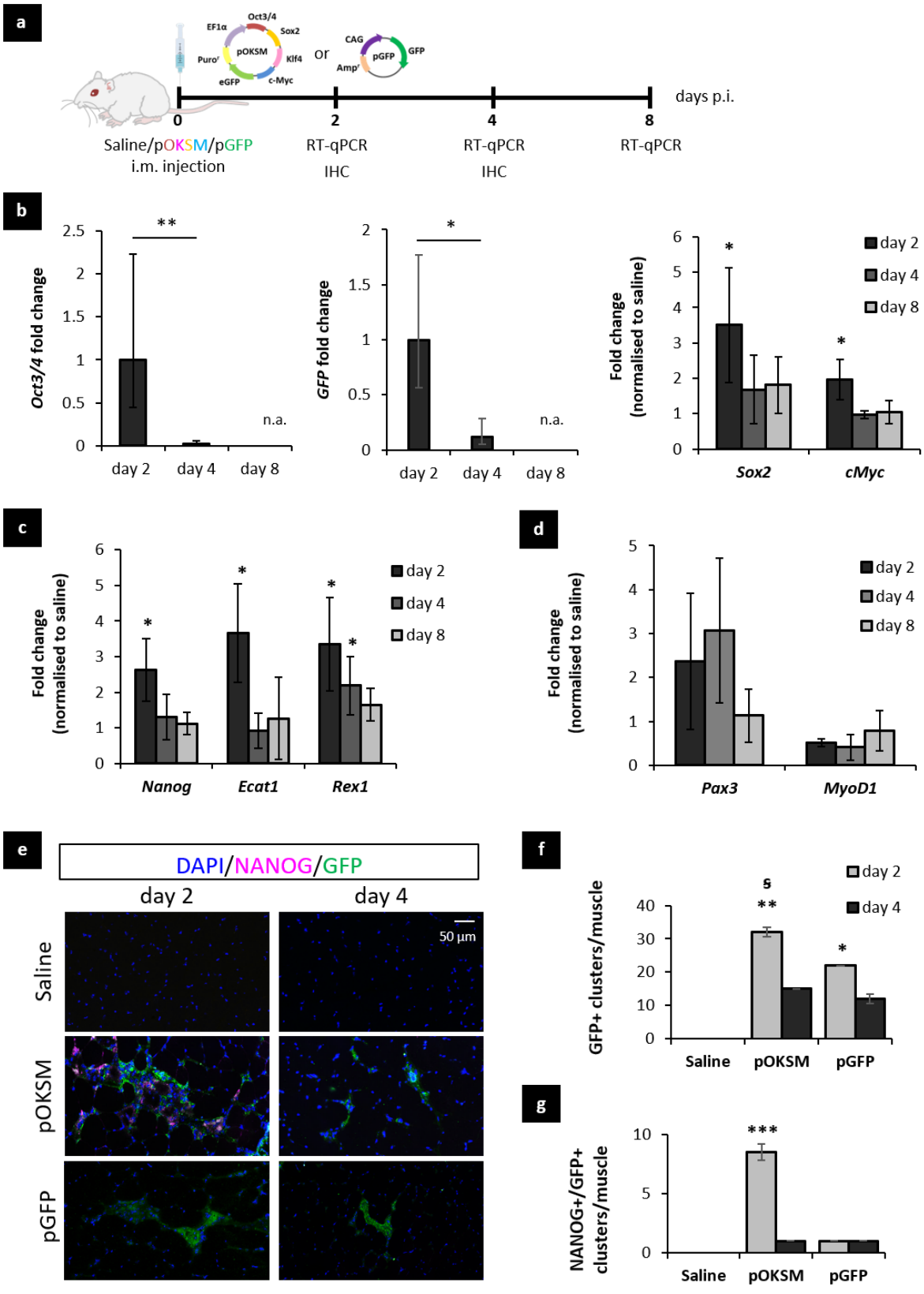
a
Oct3/4
Sox2
Klf4
c-Myc
eGFP
Puro^r
pOKSM
or
CAG
pGFP
GFP
Amp^r
days p.i.
0
2
4
8
Saline/pOKSM/pGFP
i.m. injection
RT-qPCR
IHC
RT-qPCR
IHC
RT-qPCR
b
Oct3/4 fold change
n.a.
day 2
day 4
day 8
GFP fold change
n.a.
Fold change (normalised to saline)
day 2
day 4
day 8
Sox2
cMyc
c
Fold change (normalised to saline)
day 2
day 4
day 8
Nanog
Ecat1
Rex1
d
Fold change (normalised to saline)
day 2
day 4
day 8
Pax3
MyoD1
e
DAPI/NANOG/GFP
day 2
day 4
50 µm
Saline
pOKSM
pGFP
f
GFP+ clusters/muscle
day 2
day 4
Saline
pOKSM
pGFP
g
NANOG+/GFP+ clusters/muscle
Saline
pOKSM
pGFP

Figure 2

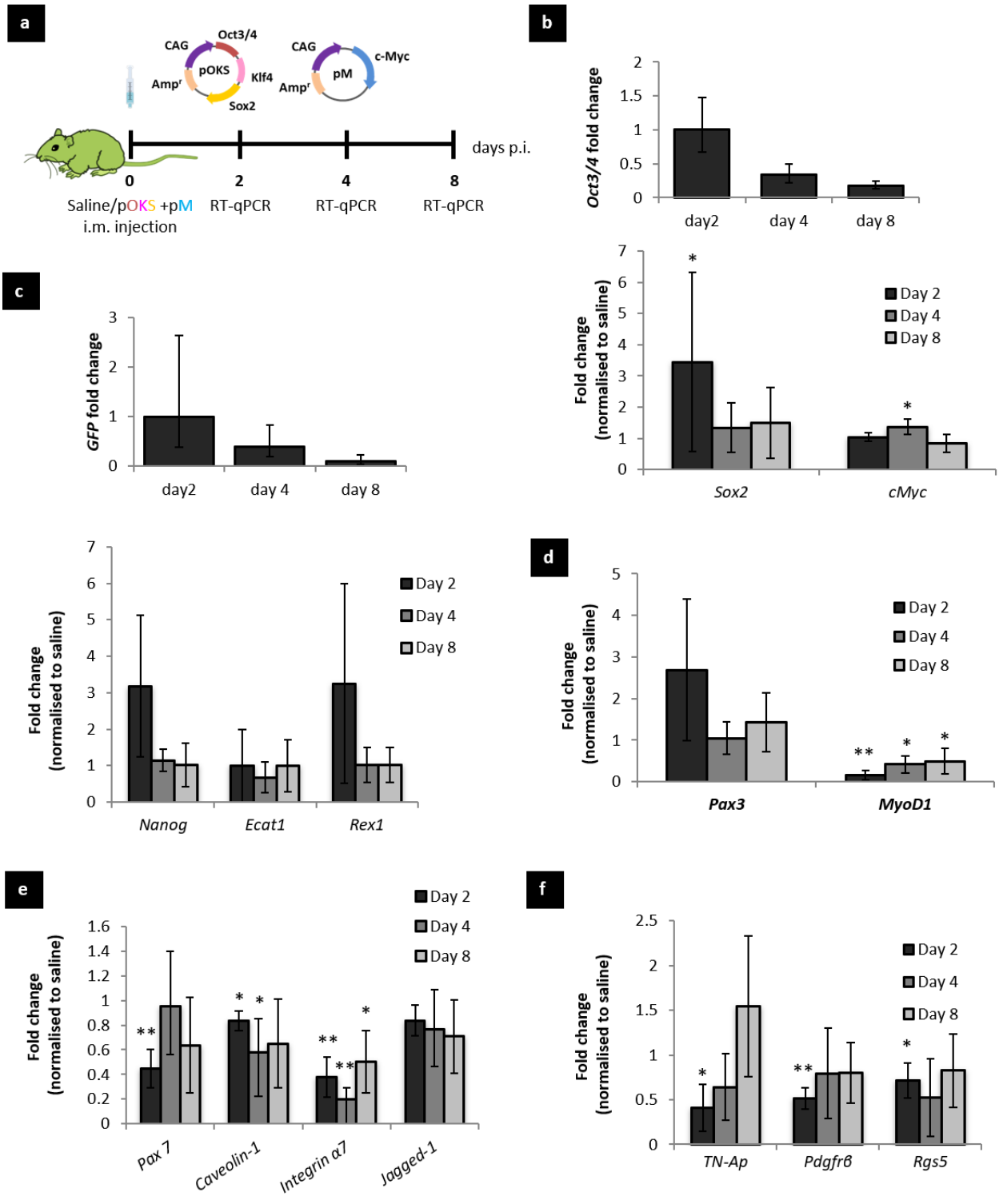
a
CAG
Oct3/4
pOKS
Klf4
Sox2
Amp^r
CAG
c-Myc
pM
Amp^r
days p.i.
0
2
4
8
Saline/pOKS +pM
i.m. injection
RT-qPCR
RT-qPCR
RT-qPCR
b
Oct3/4 fold change
day2
day 4
day 8
Fold change (normalised to saline)
Day 2
Day 4
Day 8
Sox2
cMyc
c
GFP fold change
day2
day 4
day 8
Fold change (normalised to saline)
Day 2
Day 4
Day 8
Nanog
Ecat1
Rex1
d
Fold change (normalised to saline)
Day 2
Day 4
Day 8
Pax3
MyoD1
e
Fold change (normalised to saline)
Day 2
Day 4
Day 8
Pax 7
Caveolin-1
Integrin α7
Jagged-1
f
Fold change (normalised to saline)
Day 2
Day 4
Day 8
TN-Ap
Pdgfrβ
Rgs5

Figure 3

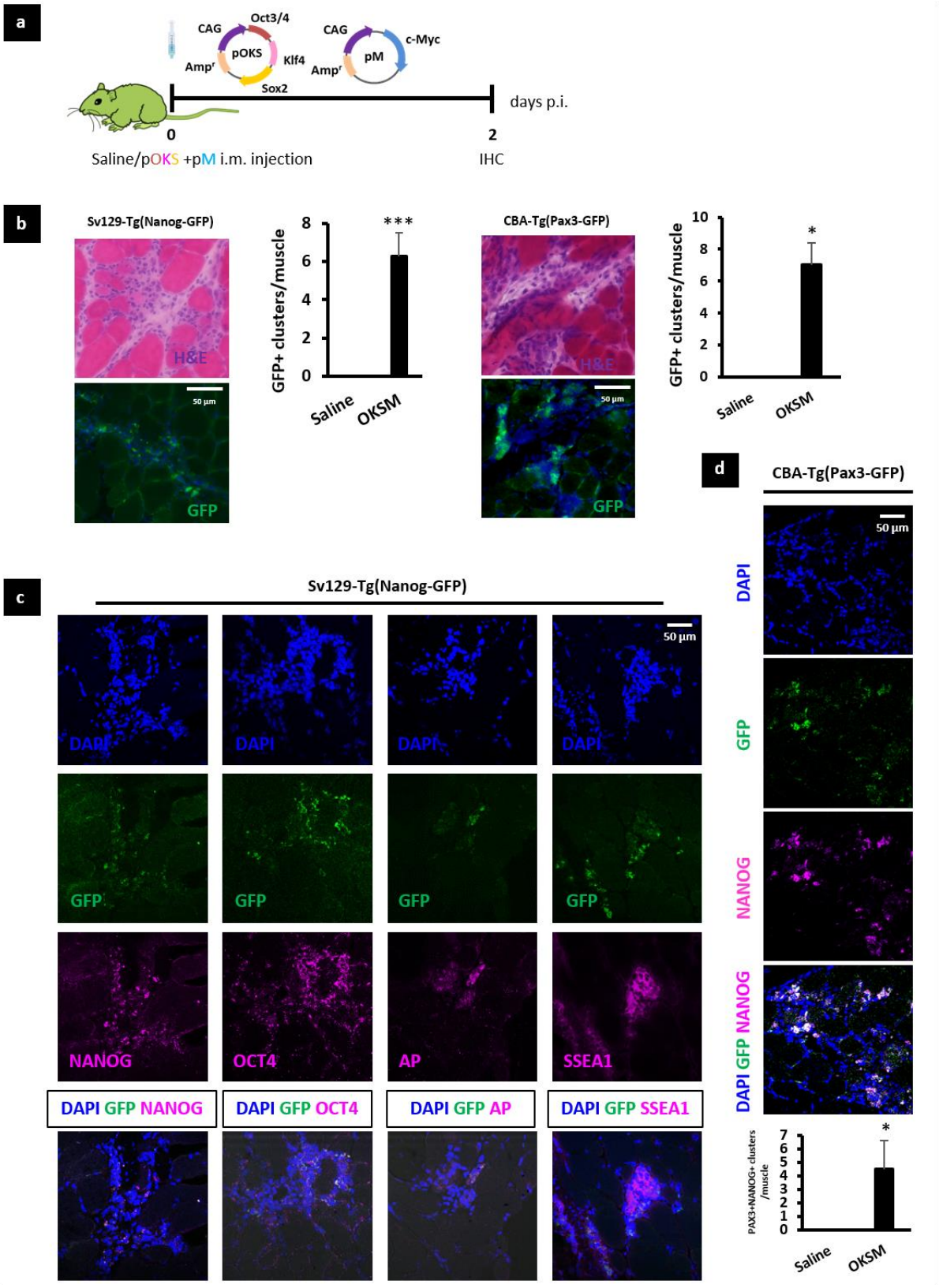
a
CAG
Oct3/4
pOKS
Klf4
Sox2
Ampr
CAG
c-Myc
pM
Ampr
days p.i.
0
2
Saline/pOKS +pM i.m. injection
IHC
b
Sv129-Tg(Nanog-GFP)
H&E
GFP
50 µm
GFP+ clusters/muscle
Saline
OKSM
CBA-Tg(Pax3-GFP)
c
Sv129-Tg(Nanog-GFP)
DAPI
GFP
NANOG
OCT4
AP
SSEA1
DAPI GFP NANOG
DAPI GFP OCT4
DAPI GFP AP
DAPI GFP SSEA1
d
CBA-Tg(Pax3-GFP)
PAX3+NANOG+ clusters /muscle

Figure 4

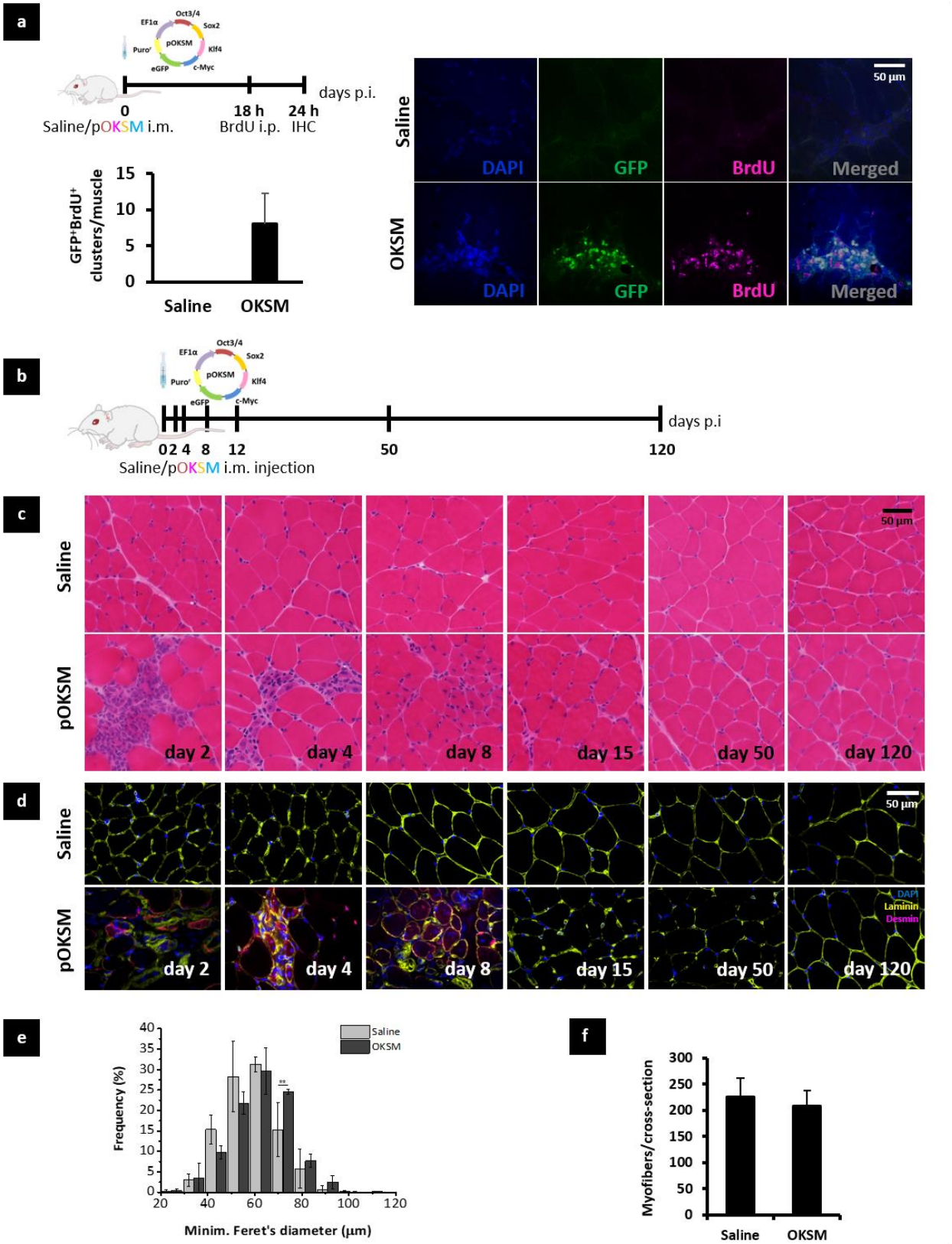
a
EF1α
Oct3/4
Sox2
pOKSM
Puro^r
Klf4
eGFP
c-Myc
days p.i.
0
18 h
24 h
Saline/pOKSM i.m.
BrdU i.p.
IHC
GFP+BrdU+ clusters/muscle
15
10
5
0
Saline
OKSM
Saline
OKSM
DAPI
GFP
BrdU
Merged
50 µm
b
days p.i
0 2 4 8 12
50
120
Saline/pOKSM i.m. injection
c
Saline
pOKSM
day 2
day 4
day 8
day 15
day 50
day 120
50 µm
d
DAPI
Laminin
Desmin
e
Saline
OKSM
Frequency (%)
Minim. Feret's diameter (µm)
f
Myofibers/cross-section
300
250
200
150
100
50
0
Saline
OKSM

Figure 5

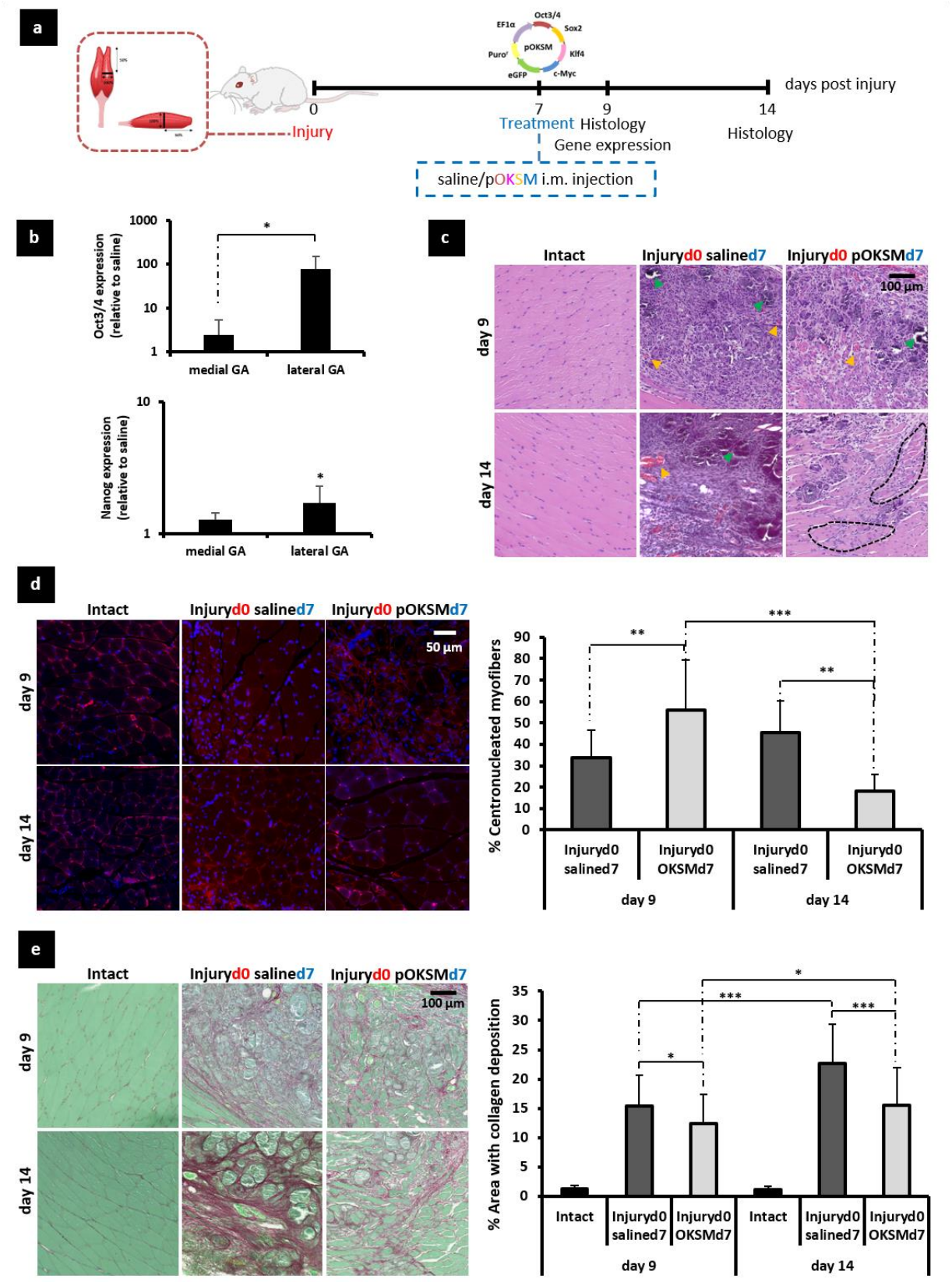
a
Oct3/4
Sox2
Klf4
c-Myc
pOKSM
EF1α
Puro'
eGFP
days post injury
0
7
9
14
Injury
Treatment
Histology
Gene expression
Histology
saline/pOKSM i.m. injection
b
Oct3/4 expression (relative to saline)
1000
100
10
1
*
medial GA
lateral GA
Nanog expression (relative to saline)
10
1
*
medial GA
lateral GA
c
Intact
Injuryd0 salined7
Injuryd0 pOKSMd7
100 µm
day 9
day 14
d
Intact
Injuryd0 salined7
Injuryd0 pOKSMd7
50 µm
day 9
day 14
% Centronucleated myofibers
90
80
70
60
50
40
30
20
10
0
**
***
**
Injuryd0 salined7
Injuryd0 OKSMd7
Injuryd0 salined7
Injuryd0 OKSMd7
day 9
day 14
e
Intact
Injuryd0 salined7
Injuryd0 pOKSMd7
100 µm
day 9
day 14
% Area with collagen deposition
35
30
25
20
15
10
5
0
*
***
***
*
Intact
Injuryd0 salined7
Injuryd0 OKSMd7
Intact
Injuryd0 salined7
Injuryd0 OKSMd7
day 9
day 14